



Contents lists available at ScienceDirect

## Soil Dynamics and Earthquake Engineering

journal homepage: [www.elsevier.com/locate/soildyn](http://www.elsevier.com/locate/soildyn)

## On the use of interstorey velocity for the seismic retrofit of steel frames with viscous dampers

Vasileia E. Logotheti, Theoni C. Kafetzi, George A. Papagiannopoulos\*, Dimitris L. Karabalis

Department of Civil Engineering, University of Patras, Patras, Greece

### ARTICLE INFO

#### Keywords:

Interstorey velocity  
Interstorey drift  
Steel frames  
Seismic retrofit  
Viscous dampers

### ABSTRACT

A simple formula is proposed that provides interstorey velocities of steel framed structures at specific interstorey drift levels. The proposed equation is statistically derived from the variation of floor relative velocity results along the height of the structure. These results are obtained by non-linear inelastic time history analyses of a number of plane steel moment resisting frames. The proposed equation can then be used for seismic retrofit purposes, i.e., in dimensioning the linear or non-linear viscous dampers to be inserted in a steel frame. A detailed numerical example is provided and conclusions regarding the accuracy and the potential use of interstorey velocity are drawn.

### 1. Introduction

The variation (distribution) of maximum interstorey velocities have been recognized as key parameter for the evaluation of the along-the-height effectiveness of and demand for viscous dampers [1]. This variation (distribution) seems to depend mainly on the modes (number of stories) of the structure under consideration.

In building codes, e.g., ASCE 7–10 [2], peak (design) interstorey velocity (IV) is approximately calculated in the fundamental and higher modes using the design (maximum) interstorey drift (IDR). This approximation permits the calculation of the maximum damping force in terms of the design IDR. Moreover, building codes, e.g., ASCE 7–10 [2], seem to accept that the most effective way of allocation of viscous dampers is to place them where large IDRs are exhibited. Therefore, the maximum IDR is used to estimate the maximum IV, without, however, providing an insight about the real relationship of maximum IDR and IV values. In literature so far, the relationship between IDR and IV is formulated either by using simplified building models and the first mode shape [3,4] or by employing single-degree-of-freedom systems and their maximum displacement [5,6]. The importance of having reliable estimates of the true IV is initially stressed by Pekcan et al. [7] in view of the operating velocities of non-linear viscous dampers and very recently by Favvata [8] in the context of seismic pounding of adjacent structures.

It is the purpose of this paper to establish a relationship between IDR and IV values for steel moment resisting frames (MRFs). More

specifically, the seismic responses in terms of floor relative displacements and relative velocities are obtained by non-linear inelastic seismic analyses of 20 plane steel MRFs under 22 real and as recorded seismic motions (accelerograms). Then, for each frame-accelerogram pair, height-wise variations of IDR and IV are constructed. Considering a specific value for IDR along-height, i.e., 1.5%, the corresponding IV values are maintained. Statistical processing of these IV values permits the derivation of an equation that provides IV along-the-height of a structure for this specific IDR.

The proposed equation is then used in a seismic retrofit scheme, where dimensioning of viscous dampers is based on IV and targets a specific IDR range. An example that involves the retrofit of a 12-storey with 4-bays, steel MRF is presented. This steel MRF is retrofitted either with linear viscous dampers or with non-linear ones. For each kind of dampers, two cases of target IDR are considered. The retrofitted MRFs are then subjected to non-linear inelastic time history analyses and IDR, IV and damper forces are computed.

On the basis of the numerical results of the present work, it can be concluded that the proposed IV equation is quite effective in satisfying target IDR. It is also demonstrated that for a specific level of seismic demand (in terms of mean acceleration spectra) the proposed IV equation offers controlled IV and IDR values as well as damper forces under the condition that plastic hinge formations to columns due to additional axial forces induced by the damper forces are within acceptable limits.

\* Corresponding author.

E-mail addresses: [Vasileia93@hotmail.com](mailto:Vasileia93@hotmail.com) (V.E. Logotheti), [kafetzi.theoni@gmail.com](mailto:kafetzi.theoni@gmail.com) (T.C. Kafetzi), [gpapagia@upatras.gr](mailto:gpapagia@upatras.gr) (G.A. Papagiannopoulos), [karabali@upatras.gr](mailto:karabali@upatras.gr) (D.L. Karabalis).

<https://doi.org/10.1016/j.soildyn.2018.07.042>

Received 5 July 2018; Received in revised form 24 July 2018; Accepted 26 July 2018

0267-7261/ © 2018 Elsevier Ltd. All rights reserved.

**Table 1**  
Subset of steel frames analyzed in this work.

Frame	Number of storeys	Number of bays	Sections: columns (HEB) – beams (IPE)
1	2	3	220 – 300 (1–2)
2	3	3	240 / 280 / 280 / 240 – 270 (1–3)
3	5	3	280 / 360 / 360 / 280 – 360 (1–2) and 260 / 360 / 360 / 260 – 330 (3–4) and 260 / 340 / 340 / 260 – 300 (5)
4	6	3	280 / 360 / 360 / 280 – 360 (1–2) and 280 / 340 / 340 / 280 – 330 (3–4) and 280 / 340 / 340 / 280 – 300 (5–6)
5	7	3	340 / 360 / 360 / 340 – 360 (1–2) and 340 / 360 / 360 / 340 – 330 (3) and 340 – 330 (4–5) and 320 – 330 (5) and 320 – 300 (6–7)
6	10	3	400 / 450 / 450 / 400 – 400 (1–2) and 360 / 400 / 400 / 360 – 400 (3–5) and 360 / 400 / 400 / 360 – 360 (6–7) and 340 / 400 / 400 / 360 – 360 (8–10)

**Table 2**  
Seismic motions used in this work.

No.	Earthquake, Location	Date	Recording Station	M <sub>w</sub>	Soil Type	PGA (m/s <sup>2</sup> )	PGV (m/s)
1.	San Fernando, U.S.A.	09/02/1971	Pacoima Dam	6.6	HR	12.03	1.12
2.	Tabas, Iran	16/09/1978	Tabas	7.1	SL	9.09	0.85
3.	Imperial Valley, U.S.A.	15/10/1979	El Centro Array 5	6.5	SL	3.72	0.91
4.	Imperial Valley, U.S.A.	15/10/1979	El Centro Array 7	6.5	SL	4.55	1.10
5.	Valparaiso, Chile	03/03/1985	Llolleo	7.9	SR	6.63	0.39
6.	Valparaiso, Chile	03/03/1985	Llaylay	7.9	SL	4.56	0.37
7.	Superstition Hills, U.S.A.	24/11/1987	Parachute Test Site	6.5	SL	4.47	1.12
8.	Loma Prieta, U.S.A.	17/10/1989	Los Gatos	7.0	HR	5.53	0.95
9.	Manjil, Iran	20/06/1990	Abbar	7.4	SR	4.87	0.52
10.	Erzincan, Turkey	13/03/1992	Erzincan	6.7	SL	5.05	0.84
11.	Petrolia, U.S.A.	25/04/1992	Cape Mendocino	6.9	HR	14.69	2.50
12.	Landers, U.S.A.	28/06/1992	Lucerne Valley	7.3	SL	7.17	1.86
13.	Northridge, U.S.A.	17/01/1994	Rinaldi Receiving St.	6.7	SL	8.22	1.66
14.	Northridge, U.S.A.	17/01/1994	Newhall	6.7	SL	5.72	0.75
15.	Northridge, U.S.A.	17/01/1994	Sylmar Converter St.	6.7	SL	6.00	1.17
16.	Kobe, Japan	17/01/1995	Takatori	6.9	SL	6.00	1.28
17.	Izmit, Turkey	17/08/1999	Sakarya	7.4	SR	3.69	0.79
18.	Chi-Chi, Taiwan	20/09/1999	TCU 052	7.6	SL	3.42	1.80
19.	El Salvador, El Salvador	13/01/2001	Santa Tecla	7.6	SR	7.28	0.41
20.	Tokachi Oki, Japan	25/09/2003	HKD 092	8.0	SL	5.70	0.53
21.	Ica Pisca, Peru	15/08/2007	ICA2	8.0	SL	3.35	0.64
22.	Christchurch, New Zealand	22/02/2011	Resthaven	6.3	SL	6.99	0.80

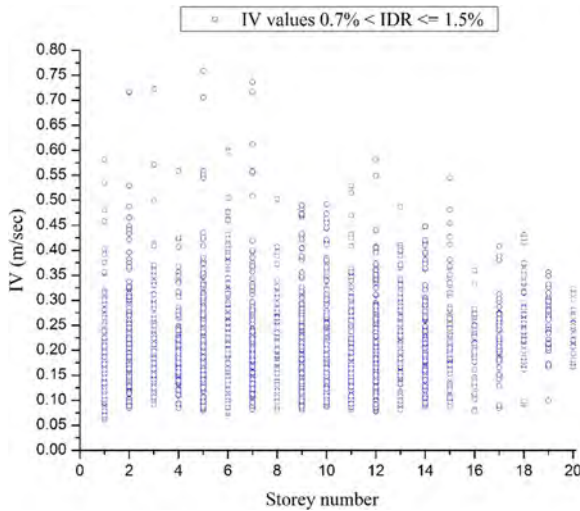


Fig. 1. IV values for 0.7% < IDR ≤ 1.5%.

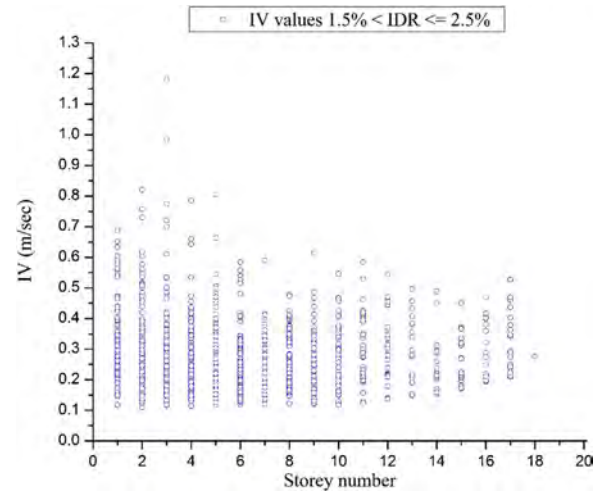


Fig. 2. IV values for 1.5% < IDR ≤ 2.5%.

**2. Seismic analyses of moment resisting steel plane frames**

**2.1. MRFs considered**

A set of 20 2-D steel MRFs is used for the parametric analyses conducted in this work. Due to space limitations and avoiding repetition, only a subset of 6 MRFs is indicatively shown in Table 1, while the remaining 14 ones of 10, 12, 13, 15, 18 and 20 storeys, can be found in

the related literature [9,10]. All considered MRFs are presented in detail in Logotheti [11].

The MRFs are orthogonal with storey height equal to 3.0 m and bay width equal to 5.0 m. The total dead and live load on beams is 27.5 kN/m. Diaphragm action is assumed at every floor due to the presence of a composite slab. The MRFs are designed according to Eurocode 3 [12] and 8 (2009), employing standard HEB, and IPE sections for columns and beams, respectively, and S275 steel grade. The design seismic load is calculated using the design spectrum of Eurocode 8 [13] with a peak

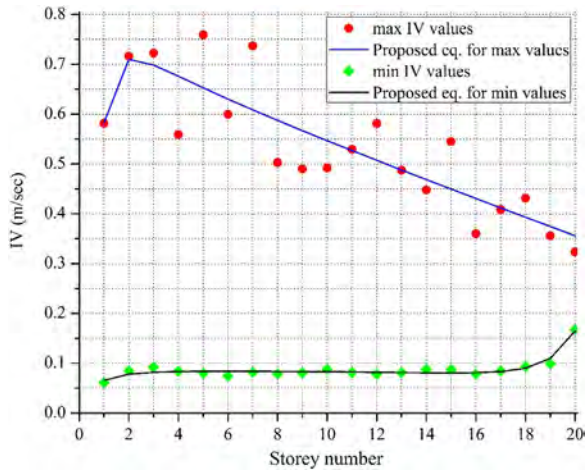


Fig. 3. Max and min IV values for 0.7% < IDR ≤ 1.5%.

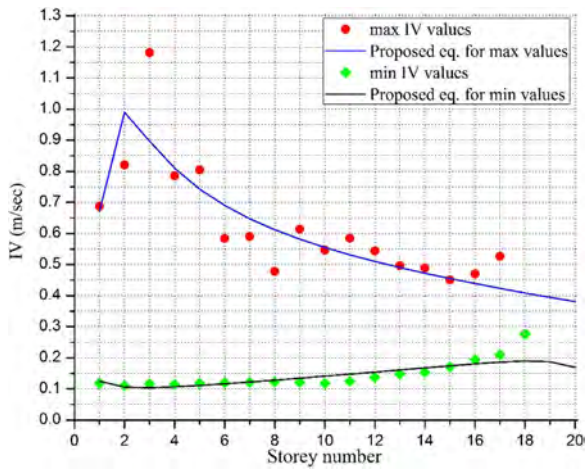


Fig. 4. Max and min IV values for 1.5% < IDR ≤ 2.5%.

**Table 3**  
Proposed equations and their correlation coefficients for max. IV.

IDR levels	Proposed equation for max IV	Correlation coefficient
IDR ≤ 0.7%	0.26	-
0.7% < IDR ≤ 1.5%	$0.703 - 0.018H + 0.274 / H - 0.377 / H^2$	0.74
1.5% < IDR ≤ 2.5%	$0.468 - 0.009H + 1.945 / H - 1.732 / H^2$	0.77
IDR > 2.5%	$0.116 + 0.009H + 2.819 / H - 2.109 / H^2$	0.85

**Table 4**  
Proposed equations and their correlation coefficients for min. IV.

IDR levels	Proposed equation for min IV	Correlation coefficient
IDR ≤ 0.7%	$0.152 - 0.006H + 7.23 \cdot 10^{-11} e^H - 0.100 / H$	0.73
0.7% < IDR ≤ 1.5%	$0.093 - 0.0007H + 1.81 \cdot 10^{-10} e^H - 0.027 / H$	0.93
1.5% < IDR ≤ 2.5%	$0.066 + 0.007H - 8.1 \cdot 10^{-11} e^H + 0.052 / H$	0.83
IDR > 2.5%	$0.105 + 0.011H - 2.7 \cdot 10^{-10} e^H + 0.068 / H$	0.82

**Table 5**  
Maximum and minimum IV values expected.

IDR levels	Maximum IV – Minimum IV (m/s)
IDR ≤ 0.7%	0.33 – 0.04
0.7% < IDR ≤ 1.5%	0.76 – 0.06
1.5% < IDR ≤ 2.5%	1.18 – 0.11
IDR > 2.5%	1.02 – 0.16

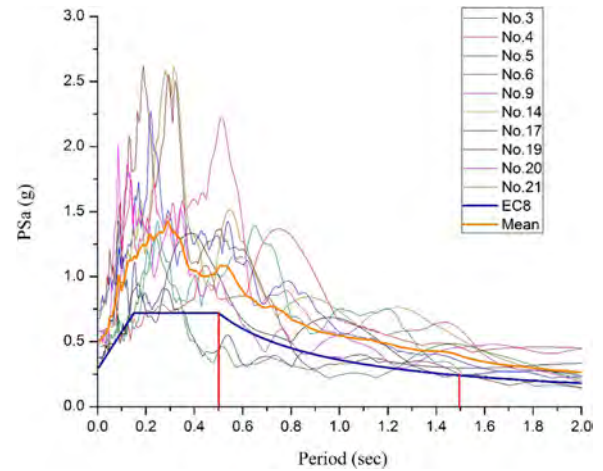


Fig. 5. 5%-damped elastic acceleration spectra.

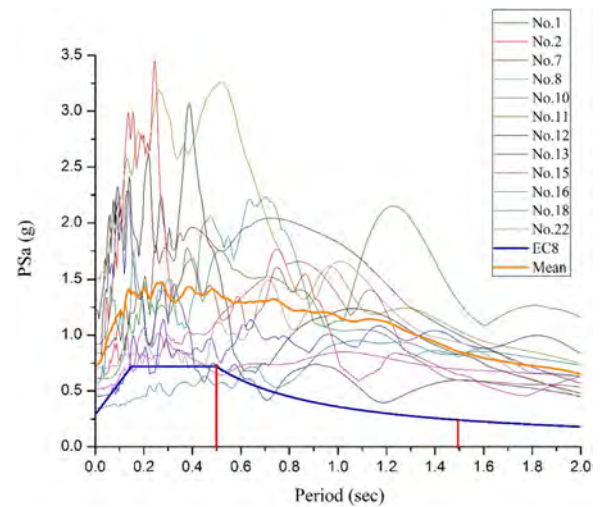


Fig. 6. 5%-damped elastic acceleration spectra.

ground acceleration (PGA) of 0.24 g, soil class B and behavior factor  $q = 3$ . Fixed-base conditions are assumed.

As shown in Table 1 section expressions of the form: i) 280 / 340 / 340 / 280 – 330 (3–4) indicate that for storeys 3 and 4 exterior and interior columns are HEB 280 and 340, respectively, and all beams are IPE 330 and ii) 340 – 330 (5) designate that for storey 5 all columns are HEB 340 and all beams are IPE 330. Column sections are oriented with their strong axis perpendicular to the plane of the MRF.

2.2. Seismic ground motions and modeling for non-linear inelastic analysis

The 22 seismic motions (accelerograms) of Table 2 are considered for the purposes of this work. These seismic motions were recorded either at the proximity of faults (near-field earthquakes) or at the broader area of subduction zones. According to the opinion of the authors, the seismic motions of Table 2 represent cases of very strong

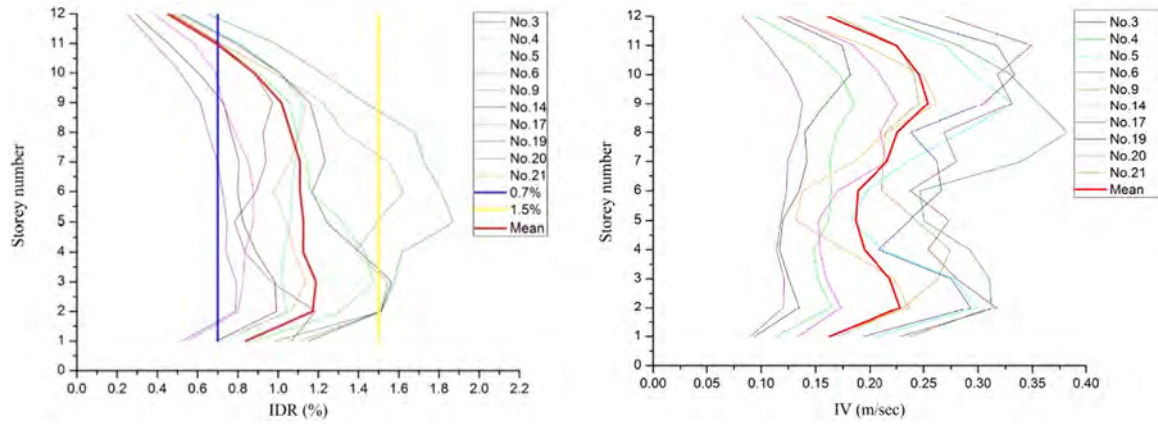


Fig. 7. IDR and IV values before retrofitting– set I-).

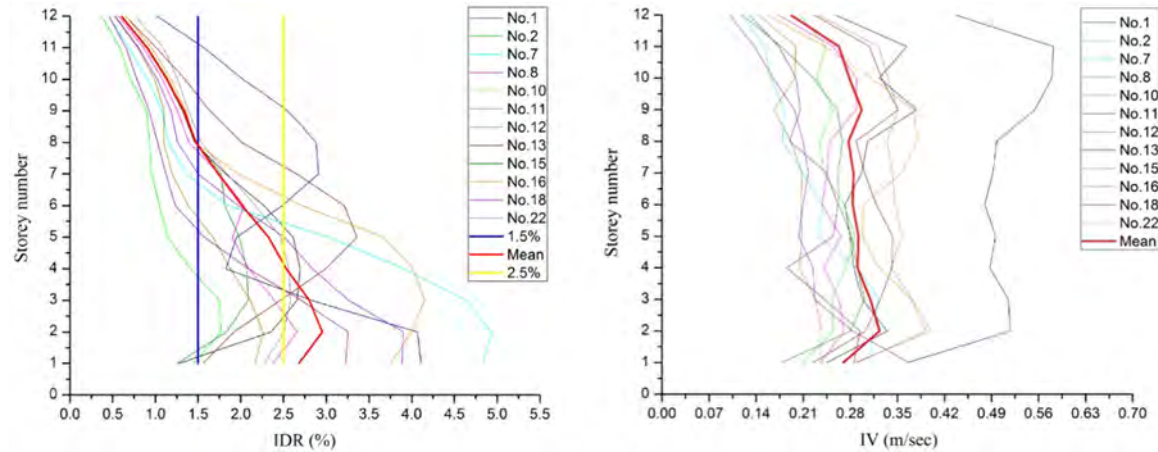


Fig. 8. IDR and IV values before retrofitting– set II-).

earthquake ground motion and as such can force the steel MRFs in the nonlinear inelastic regime. Several details about these seismic motions concerning location, date, recording station, moment magnitude  $M_w$ , soil type, PGA and peak ground velocity (PGV) can also be found in Table 2. Regarding soil type, the abbreviations HR, SR and SL correspond to hard rock, sedimentary and conglomerate rock and soil / alluvium, respectively.

For the execution of the non-linear inelastic analyses, beams and columns are modelled using standard frame elements with concentrated plasticity and 2% strain hardening. Axial-flexural interaction is considered for the plastic hinges of the columns. Direct modeling of panel zone effect is not required as requirements of ASCE 41–13 [14] are satisfied, whereas the steel strength cyclic degradation effect is ignored in view of future investigation. The inherent viscous damping of each steel MRF is considered to be 3% of critical for the first mode of vibration and for that mode for which the participation of the effective modal mass is 90%.

### 3. Derivation and use of the IV equation

For the aforementioned 20 steel frames subjected to the 22 accelerograms of Table 2, the relative to the ground motion velocity and displacement of each floor are obtained by non-linear inelastic seismic analyses using SAP2000 [15]. The height-wise variation in terms of IDR and IV is then computed for each frame-accelerogram combination. Considering specific IDR levels, i.e.,  $IDR \leq 0.7\%$ ,  $0.7\% < IDR \leq 1.5\%$ ,  $1.5\% < IDR \leq 2.5\%$  and  $IDR > 2.5\%$ , plots involving IV and storey number are constructed. Due to space limitations, only the plots for  $0.7\% < IDR \leq 1.5\%$  and  $1.5\% < IDR \leq 2.5\%$  are shown in Figs. 1, 2

respectively. The rest two plots, for the other two aforementioned IDR levels, can be found in Logotheti [11]. It should be also noted that the 0.7%, 1.5%, 2.5% are established IDR values regarding the seismic performance of steel MRFs and can be found in the pertinent literature (e.g. [16]).

Isolating the maximum and minimum values from the plots involving IV and storey number (i.e. Figs. 1, 2), one has plots in the form of Figs. 3, 4. In these plots, the IV values do not correspond to the same value of IDR but are essentially within the selected IDR level, i.e.  $0.7\% < IDR \leq 1.5\%$  and  $1.5\% < IDR \leq 2.5\%$ . Thus, the maximum and minimum values shown in Figs. 3, 4 represent upper and lower limits for IV, respectively. In an attempt to interpolate the upper and lower bounds of IVs, the following equations are proposed

$$\max. IV = a + b \cdot H + c/H + d/H^2 \quad (1)$$

$$\min. IV = a + b \cdot H + c \cdot e^H + d/H \quad (2)$$

where, a-d are constants and H is the storey number ( $1 \leq H \leq 20$ ). Values for these constants as well as the correlation coefficients for these equations have been tabulated in Tables 3, 4. Standard errors as well as 95% confidence limits for the constants a-d are reported in Logotheti [11]. Plots of the proposed equations are also shown in Figs. 3, 4.

It should be stressed that even though more complicated expressions, involving a larger number of constants, can be constructed for a closer applied and fit to the computed IV values, it is decided, for simplicity, to keep the number of constants to a minimum, i.e., up to 4. Moreover, the correlation coefficient of the proposed equations should not be less than 0.70.

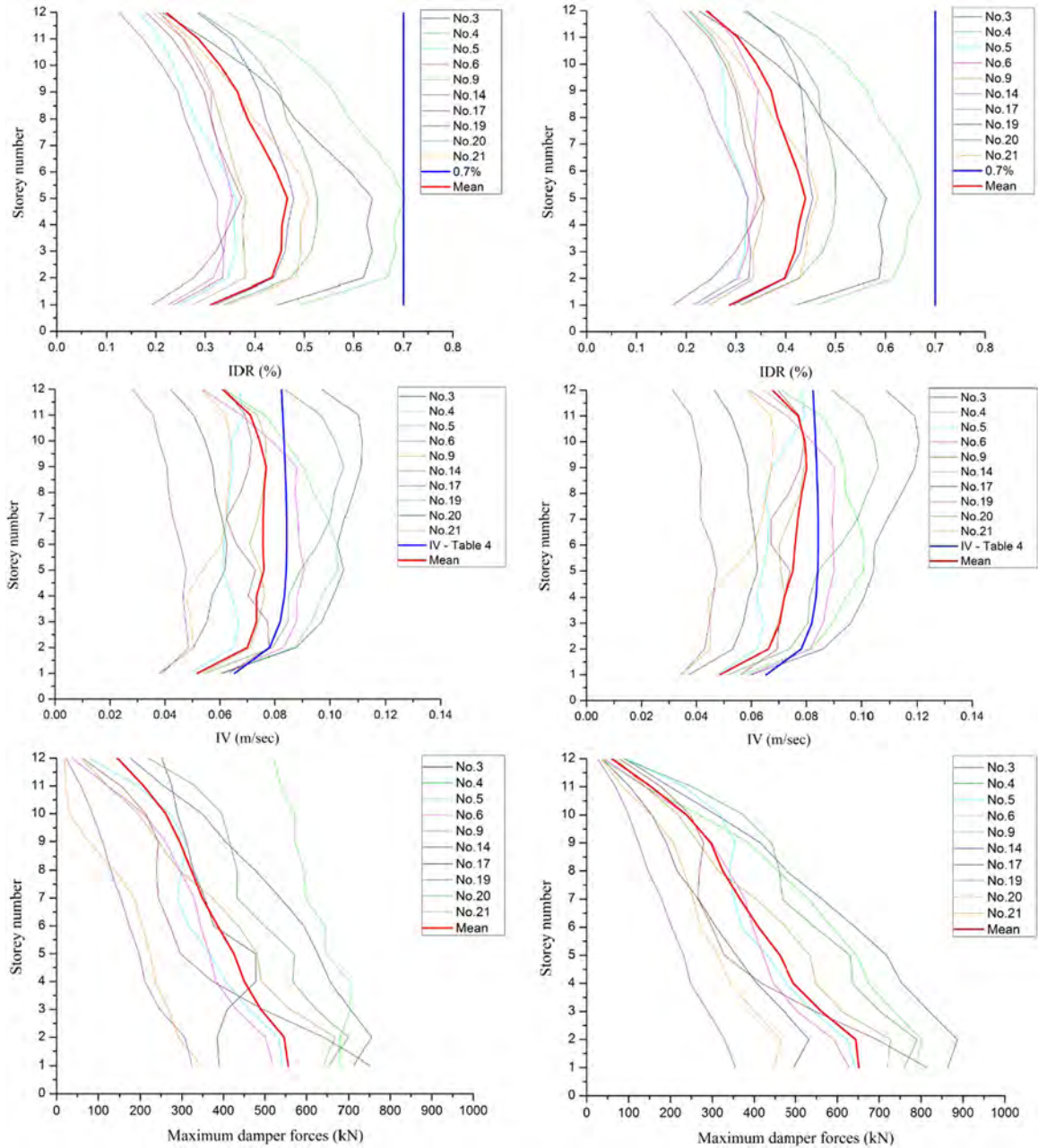


Fig. 9. IDR, IV values and maximum damper forces for  $k = 0.8$  (left) and  $k = 1.0$  (right) – set I- &  $\alpha = 1.0$ .

For the case of  $IDR \leq 0.7\%$ , no proper expression in the form of Eq. (1) is found and, therefore, the mean constant IV value 0.26 is chosen. The proposed Eqs. (1) and (2) can be used as estimates for maximum and minimum expected IV values for specific IDR levels of MRFs, and, thus, avoiding time and resource demanding non-linear inelastic seismic analyses.

It is anticipated that values of IV for  $IDR \leq 0.7\%$  correspond to elastic behavior of the MRF, whereas values of IV for  $IDR > 0.7\%$  essentially to inelastic behavior. The maximum and minimum IV values computed from the previous non-linear inelastic analyses, irrespectively of the floor level in which they appear, are summarized in Table 5. Overlaps of IV values are evident from Table 5. Similarly, overlaps are also observed if maximum and minimum IV values are calculated from the equations given in Tables 3, 4. Table 5 also reveals that the IV range for  $1.5\% < IDR \leq 2.5\%$  encloses the corresponding one for  $IDR > 2.5\%$ . But most importantly, Table 5 reveals that due to the aforementioned overlaps, the maximum IV values do not guarantee a single

IDR range.

Taking into account that damper forces are related to IV values, dimensioning of a linear or non-linear viscous damper in terms of its damping coefficient  $C$ , can be performed using the Eq. (3) which originates from the typical diagonal brace configuration in a steel frame.

$$C = k \cdot V_{storey} / (IV^\alpha \cdot \cos^2\theta) \quad (3)$$

In Eq. (3),  $V_{storey}$  is the storey shear force,  $k$  is a factor that expresses the storey shear force that should be resisted by the viscous damper,  $\alpha$  is the velocity exponent (equals to 1 for a linear damper and less than 1 for a non-linear one) and  $\theta$  is the angle of inclination of the damper.

On the basis of Eq. (3) and of the previous discussion regarding Table 5, for the retrofit of a MRF with viscous dampers, the minimum IV values of Table 4 should be used. This way increased values of the damper coefficient  $C$  will be obtained, leading thus to increased damping ratios of the MRF. At this point, one should also mention that the minimum IV values of Table 4 are less than unity resulting in higher

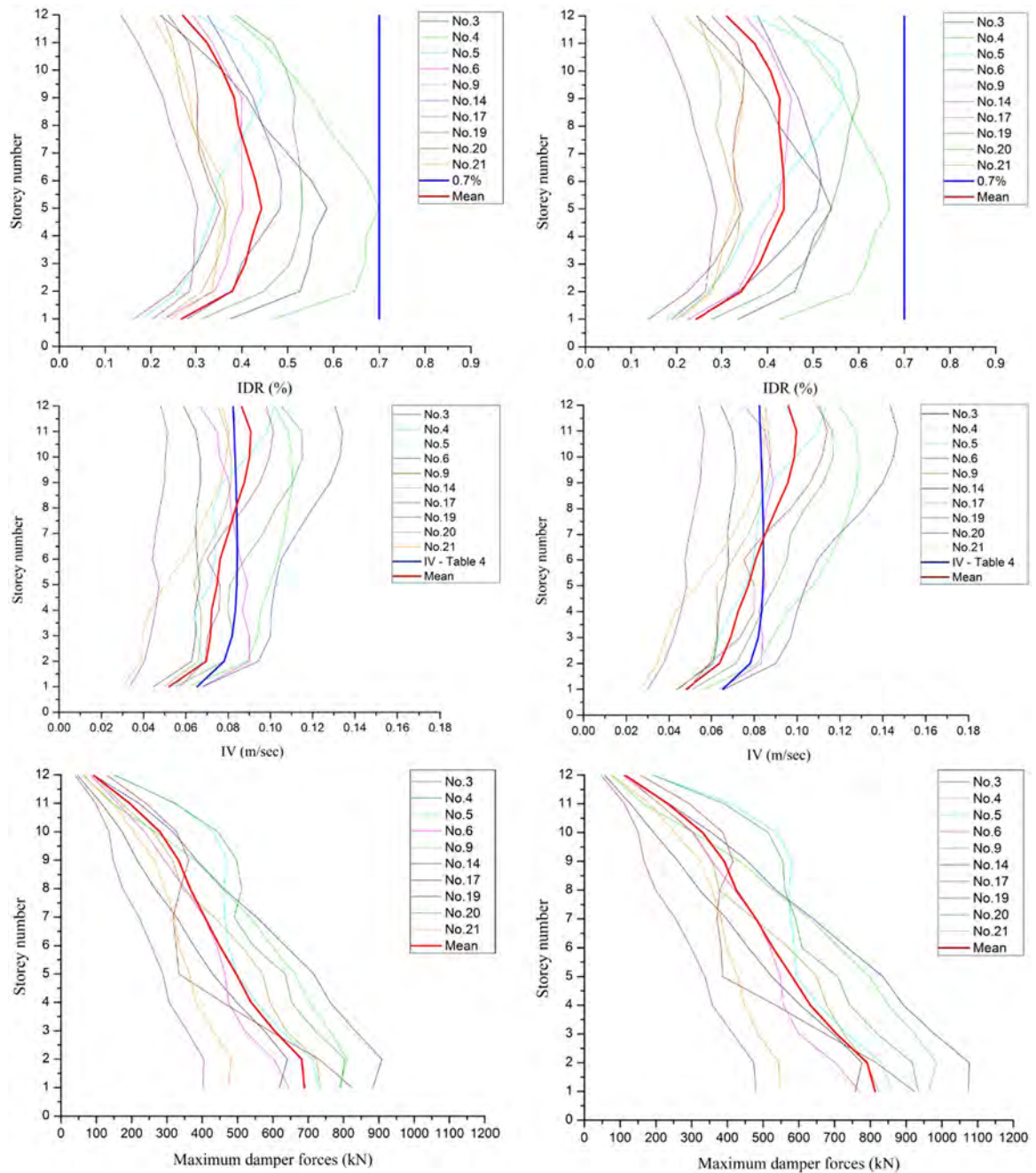


Fig. 10. IDR, IV values and maximum damper forces for  $k = 0.8$  (left) and  $k = 1.0$  (right) – set I- &  $\alpha = 0.6$ .

denominator values with decreasing values of the exponent  $\alpha$  for a specific IV value. For fixed value of the nominator, the damper coefficient of a non-linear damper  $C^{NON}$  can be related to the corresponding one of a linear damper  $C^{LIN}$  via Eq. (4) which reveals that for a specific IV value  $C^{NON}$  is always less than  $C^{LIN}$ .

$$C^{NON} = C^{LIN} \cdot IV^{1-\alpha} \quad (4)$$

Employing Eq. (3) and setting the desired seismic performance, if retrofit targets elastic behavior for the MRF, dimensioning of the linear or non-linear dampers can be performed using the IV values for the case of  $IDR \leq 0.7\%$  of Table 4. Alternatively, retrofit should target at least to the case  $0.7\% < IDR \leq 1.5\%$  by using the IV values of Table 4 that correspond to this IDR range. For this retrofit case, the MRF will most likely exhibit minor inelastic behavior and the strength and stroke limits of the dampers are not expected to be surpassed. Moderate to large inelastic behavior is anticipated for the cases  $1.5\% < IDR \leq$

$2.5\%$  and  $IDR > 2.5\%$ , and the strength and stroke limits of the dampers may be surpassed.

#### 4. USE of IV in seismic retrofit of a MRF with viscous dampers

The proposed IV expressions are employed herein for the retrofit of a 12-storey (storey height is 3.0 m) and 4-bay (bay width is 4.0 m) steel MRF with viscous dampers [17]. This steel MRF resembles the geometrical, loading and design patterns of the frames presented in Section 2.1, but it is not identical to any of the 20 steel MRFs used for the parametric analyses discussed earlier. Non-linear inelastic time history analysis, considering an inherent 3% viscous damping, of the aforementioned steel MRF is performed employing the 22 seismic motions of Table 2. IDR, IV and maximum storey shear forces are obtained for each seismic motion.

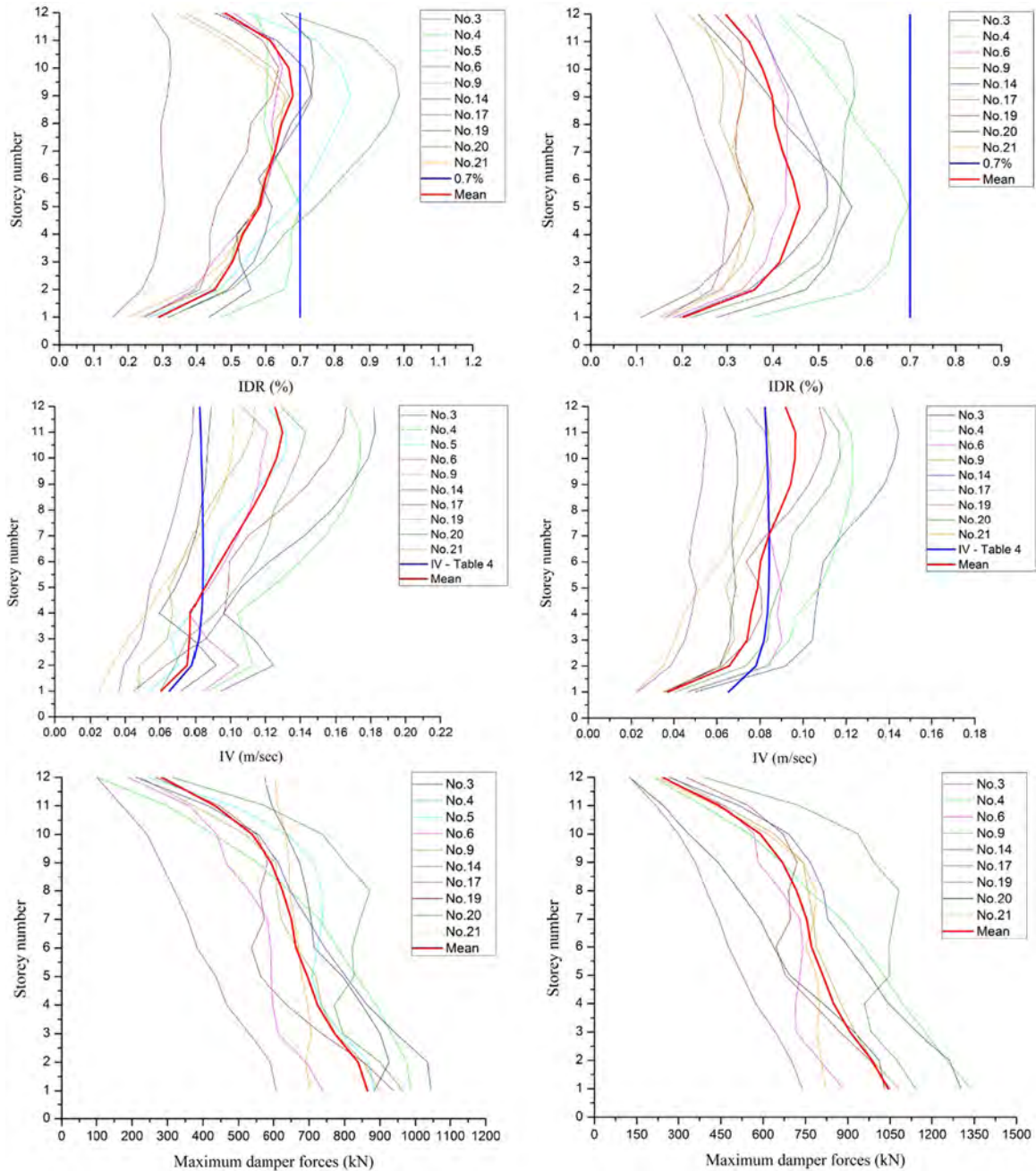


Fig. 11. IDR, IV values and maximum damper forces for  $k = 0.8$  (left) and  $k = 1.0$  (right) – set I- &  $\alpha = 0.2$ .

A comparative study is initially conducted for the steel MRF in which all dampers are installed in a diagonal configuration either at the interior or at the exterior bays. The outcome of this study indicates that dampers are marginally more efficient if they are installed in the interior bays. On the other hand, regarding the size (force capacity) of the viscous dampers required, it is true that dampers of large size increase the cost of retrofit. Therefore, it is decided to install dampers of smaller size, at the outer bays and at all storeys, increasing thereby the already high axial force demands of the outer columns of the steel MRF. Smaller size dampers have also the advantages of simplified connections of the dampers to the MRF and of avoiding axial load accumulation in its columns [18]. It should be also noted that the dampers should essentially have the same size in order to avoid the cost of testing different dampers for a single retrofit project [19].

Considering then that: a) all viscous dampers can be either linear ( $\alpha = 1.0$  in Eq. (3)) or non-linear ( $\alpha = 0.2$  or  $0.6$  in Eq. (3)), b) the

viscous dampers should resist 80% or 100% of the total storey shear force ( $k = 0.8$  or  $1.0$  in Eq. (3)) and c) retrofit targets either  $IDR \leq 0.7\%$  or  $0.7\% < IDR \leq 1.5\%$ , one can make use of the corresponding min. IV equations of Table 4 and estimate the damping coefficients of the linear dampers from Eq. (3) and of the non-linear dampers from either Eq. (3) or Eq. (4). It should be also reminded that the incorporation of the viscous dampers corresponding to a reasonable added damping ratio of 5–20% in the MRF, introduces usually negligible influence on its fundamental period for excitation frequencies ranging from 0 to 3 Hz [20].

Subsequently, the steel MRF retrofitted with viscous dampers is re-subjected to the 22 seismic motions of Table 2 and seismic response results in terms of IDR, IV and of the forces on viscous dampers are computed. For the non-linear inelastic analyses of the retrofitted MRF, linear or non-linear viscous dampers are modelled as discrete damping elements using the 'Link element' of SAP2000 [15]. However, a detailed

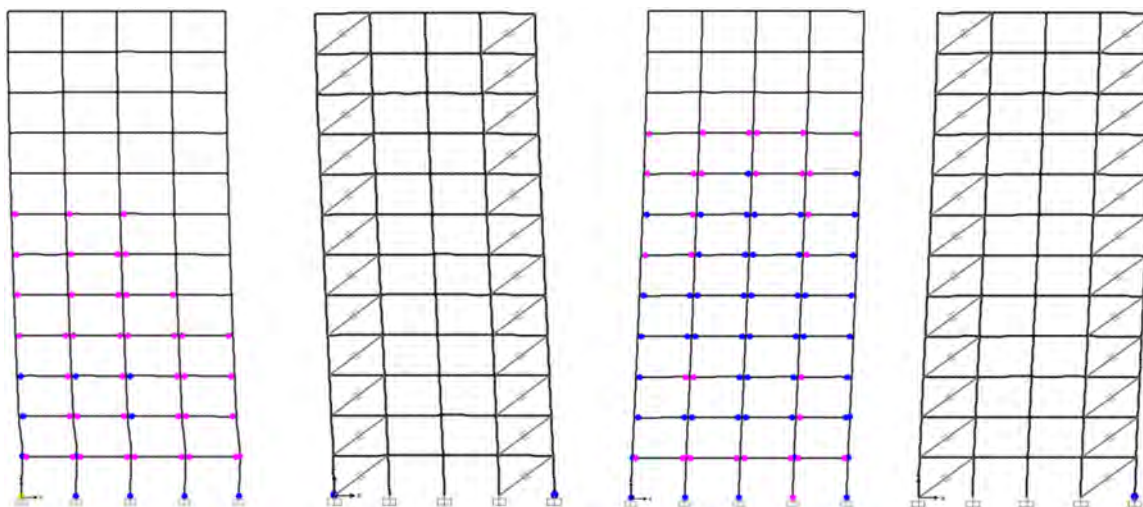


Fig. 12. Plastic hinge formations before and after the addition of linear dampers for the seismic motions No.4 (left) and No.20 (right) of set I-.

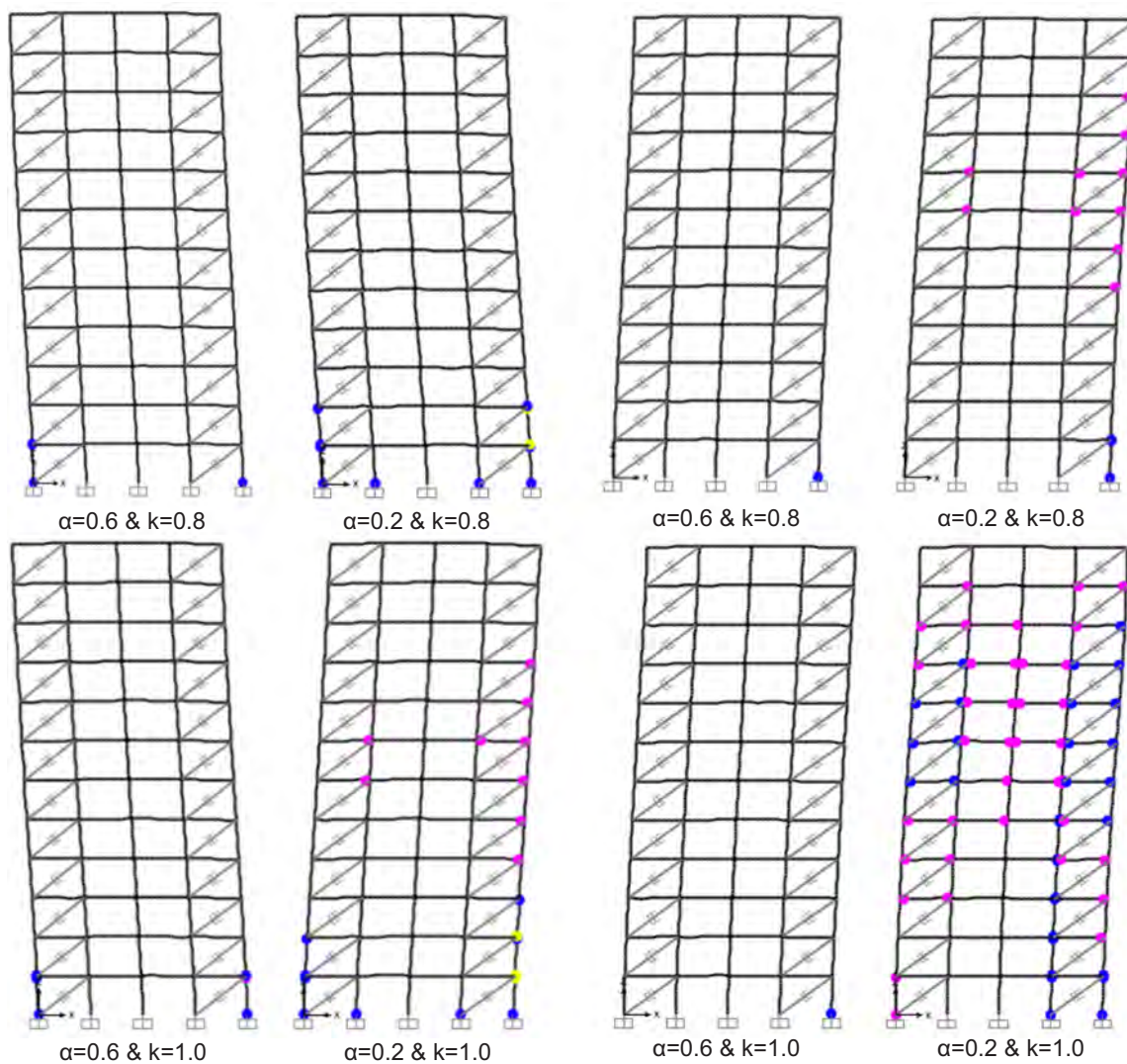


Fig. 13. Plastic hinge formations after the addition of non-linear dampers for the seismic motions No.4 (left) and No.20 (right) of set I-.

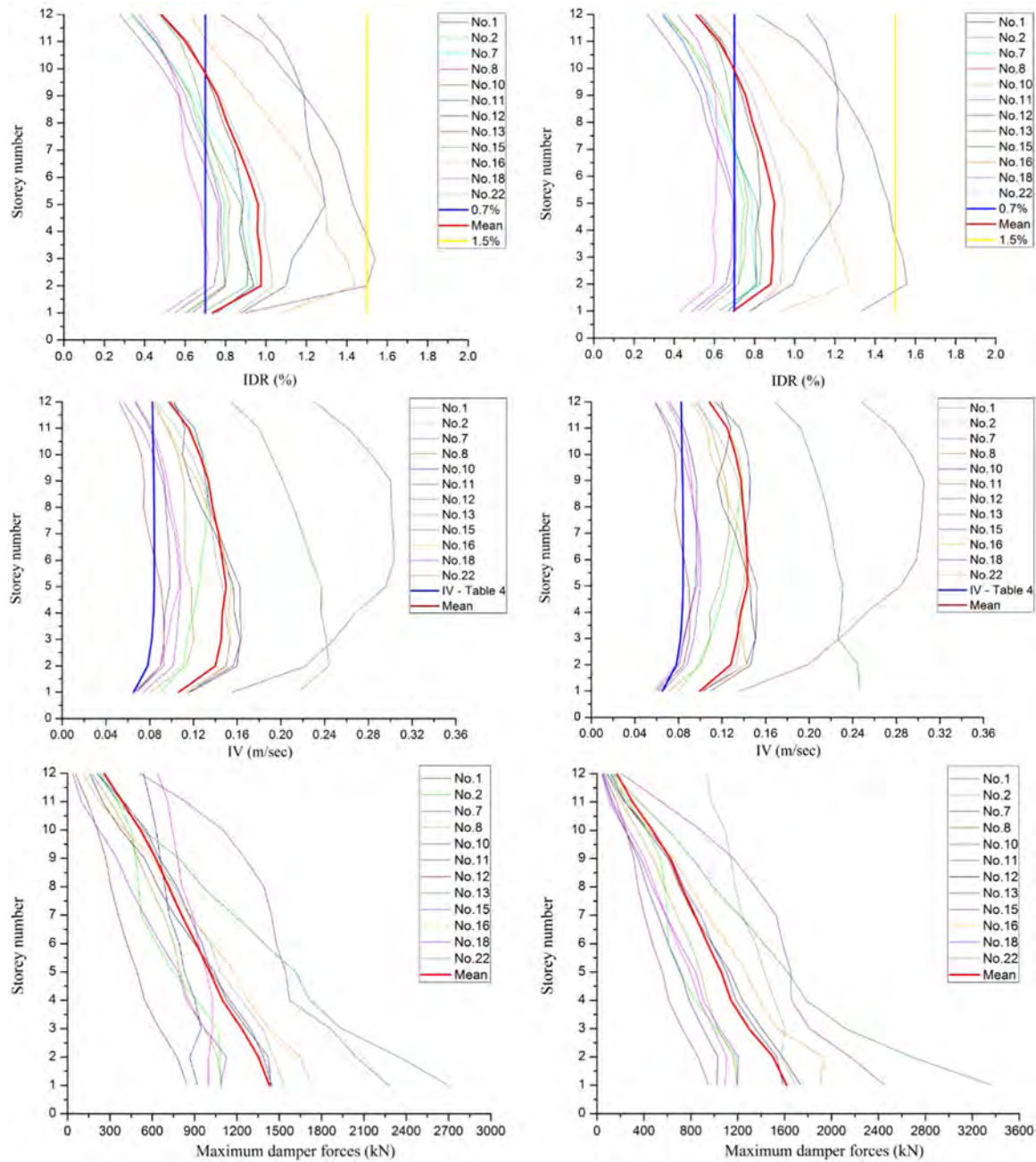


Fig. 14. IDR, IV values and maximum damper forces for  $k = 0.8$  (left) and  $k = 1.0$  (right) – set II-) &  $\alpha = 1.0$ .

modeling and limit states for dampers [21,22] are not taken into account in view of the fact that the collapse performance of the MRF is out of the scope of the present work. Nevertheless, as it is demonstrated in the following, the increase of axial forces in columns due to damper forces may significantly affect the collapse potential of the retrofitted MRF.

Before the presentation of numerical results, a short discussion is due regarding the set of the seismic motions (accelerograms) used in terms of expected seismic demand, following Uriz and Whittaker [23] and Wang and Mahin [18]. These seismic motions are separated into two sets: I-) No. 3–6, 9, 14, 17, 19–21 (10 in total) and II-) the remaining ones according to Table 2 (12 in total). It is assumed that these sets represent two levels of seismic demand in terms of their mean 5%-damped elastic acceleration spectra. These mean spectra along with the individual 5%-damped elastic response spectra of the accelerograms of Table 2 and the 5%-damped elastic design spectrum of Eurocode 8 [13]

used for the design of the MRF under study, are shown in Figs. 5, 6.

Referring to Fig. 5, and focusing on the individual spectral ordinates at the periods of interest (shown with vertical lines), i.e., the first two modes of the steel MRF under study, one may find that the acceleration corresponding to seismic motions of set I-) compared to the design acceleration of EC8 satisfies a ratio between 1.0 and 2.0. Considering the 5%-damped mean spectrum of the seismic motions of set I-), one gets for the same periods of interest, that the ratio of the mean to design acceleration is 1.47 for  $T = 0.5$  s and 1.62 for  $T = 1.5$  s. Thus, it is expected that for the seismic motions of set I-), the retrofit using viscous dampers (essentially offer at least 5% more viscous damping to the inherent 3% of the MRF) will be successful leading to elastic or mildly inelastic response of the MRF.

On the contrary, as it is shown in Fig. 6, the ordinates of the 5%-damped mean spectrum of the seismic motions of set II-), substantially exceed those of the design spectrum for periods greater than 0.3 s. More

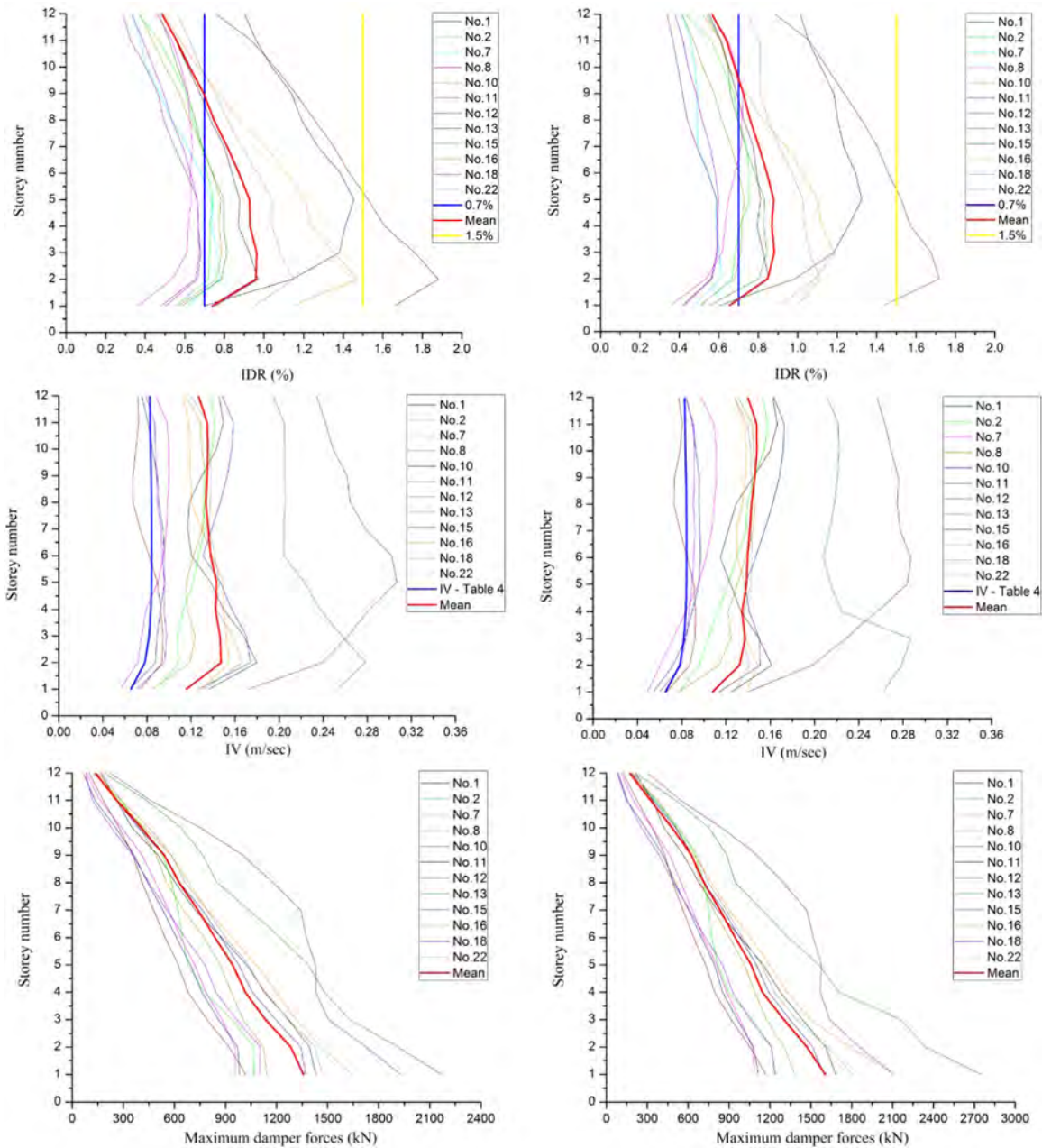


Fig. 15. IDR, IV values and maximum damper forces for  $k = 0.8$  (left) and  $k = 1.0$  (right) – set II-) &  $\alpha = 0.6$ .

specifically, the ratio of the mean to design acceleration is 1.93 for  $T = 0.5$  s and 3.54 for  $T = 1.5$  s, thus, even in the presence of increased damping (at least 5% more viscous damping to the inherent 3% of the MRF is provided by the viscous dampers), the MRF is expected to exhibit medium to large inelastic response. Thus, it can be said that set II-) represents a higher seismic demand level (in terms of a mean acceleration spectrum) than set I-).

## 5. Results for the retrofitted frame and discussion

Taking into account the aforementioned spectral considerations, detailed results from non-linear inelastic time-history analyses are presented in the following. The results involve IDR and IV values for the retrofitted MRF as well as maximum forces of the viscous dampers. For comparison purposes, mean IDR and IV values as well as target IDR and the IV values from Table 4 are also shown.

Results will be presented separately for sets I-) and II-). For each set,

according to ASCE 7–10 [2] and its subsequent modifications, mean values are permitted to be used since at least seven seismic motions are used. To highlight the need of placing dampers, the IDR and IV responses of the MRF before retrofitting are provided in Figs. 7–8 for the seismic motions of set I-) and II-), respectively. Mean IDR and IV values are also shown in Figs. 7–8 and on the basis of the mean IDR values, it is considered that retrofit targets  $IDR \leq 0.7\%$  for set I-) and  $0.7\% < IDR \leq 1.5\%$  for set II-). The damping coefficients  $C$  of the viscous dampers are obtained using Eqs. (3) and (4) (for  $k = 0.8$  or  $1.0$ ), where the IV expression of Table 4 for the case  $0.7\% < IDR \leq 1.5\%$  is employed due to its better correlation coefficient in comparison to the equation used for  $IDR \leq 0.7\%$ .

Response results are presented first for set I-). Figs. 9–11, display, for  $\alpha = 1.0, 0.6$  and  $0.2$ , respectively, the height-wise variation of IDR, IV and the maximum damper forces for the two values of  $k$ . Mean values for IDR, IV and damper forces as well as target IDR (0.7%) and IV (from Table 4) values are also shown in Figs. 9–11. Worst plastic hinges

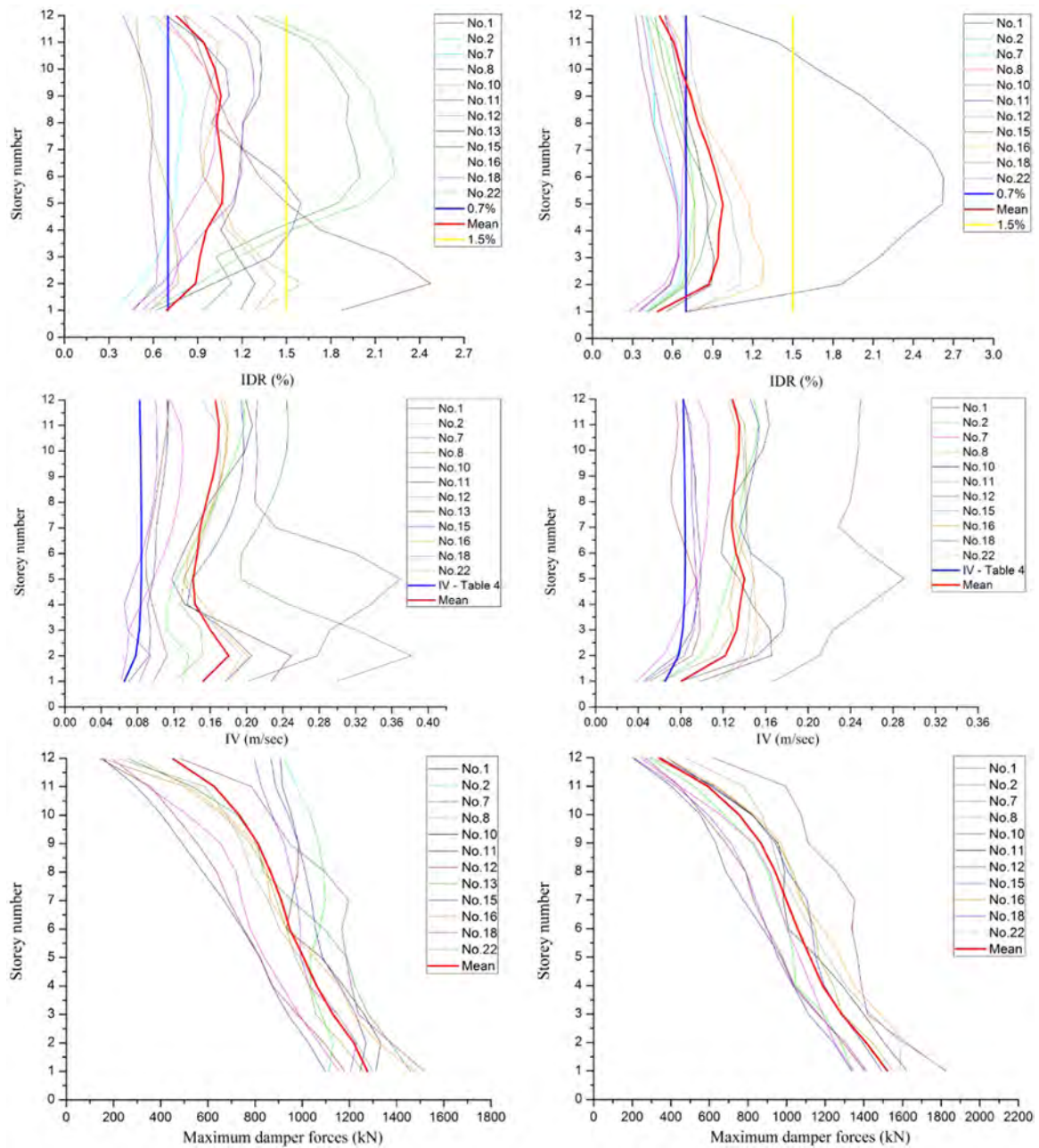


Fig. 16. IDR, IV values and maximum damper forces for  $k = 0.8$  (left) and  $k = 1.0$  (right) – set II-) &  $\alpha = 0.2$ .

formations before and after the addition of linear and non-linear dampers, are identified for the seismic motions 4 and 20 of set I-) and are shown in Figs. 12–13 for the two values of  $k$ . For the case of linear dampers (Fig. 12), these worst plastic hinge formations for the seismic motions 4 and 20 are found to be the same, irrespectively of the value of  $k$ . Nevertheless, it should be noted that for the seismic motion No.5 with  $k = 1$  and  $\alpha = 0.2$ , response cannot be computed due to excessive number of plastic hinges.

From Figs. 9–13, one can conclude that: i) for the case of linear dampers mean IDR and IV values satisfy their target values; ii) for the case of non-linear dampers with  $\alpha = 0.6$ , mean IDR values satisfy the target values, whereas mean IV values satisfy their target values for the first 7 (for  $k = 1.0$ ) and 8 (for  $k = 0.8$ ) storeys; iii) for the case of non-linear dampers with  $\alpha = 0.2$ , mean IDR values satisfy the target values, whereas mean IV values satisfy their target values for the first 7 (for  $k = 1.0$ ) and 4 (for  $k = 0.8$ ) storeys; iv) for all damper cases, as expected, the mean maximum damper forces for  $k = 0.8$  are lower than

those for  $k = 1.0$ .

For all seismic motions of set I-), the addition of linear dampers to the MRF is effective in reducing IDR, IV and number of plastic hinges in comparison to the initial MRF without dampers. On the other hand, the addition of non-linear dampers to the MRF is effective in reducing IDR and IV in comparison to the initial MRF without dampers, however, plastic hinge formations may take place in few or many elements but in a different pattern than the expected one. More specifically, for two of the seismic motions of set I-), significant increases in axial forces of columns occurred due to the forces induced by the non-linear dampers, leading to undesired plastic hinge formations at the top end of the columns of the first lower storeys. The number of these undesired plastic hinges to columns depends on the values of  $\alpha$  and  $k$  and seems to increase as the velocity exponent decreases.

End plastic rotations, according to ASCE 41–13 [14] lie within: i) the range of immediate occupancy (IO) and life safety (LS) limit states for the case of linear dampers and involve only the columns of the first

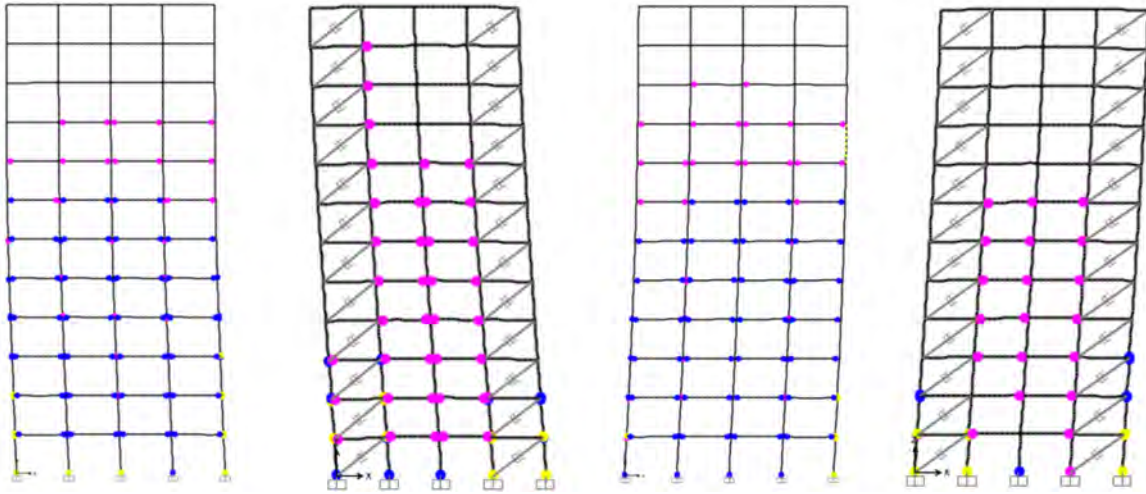


Fig. 17. Plastic hinge formations before and after the addition of linear dampers for the seismic motions No.16 (left) and No.22 (right) of set II-).

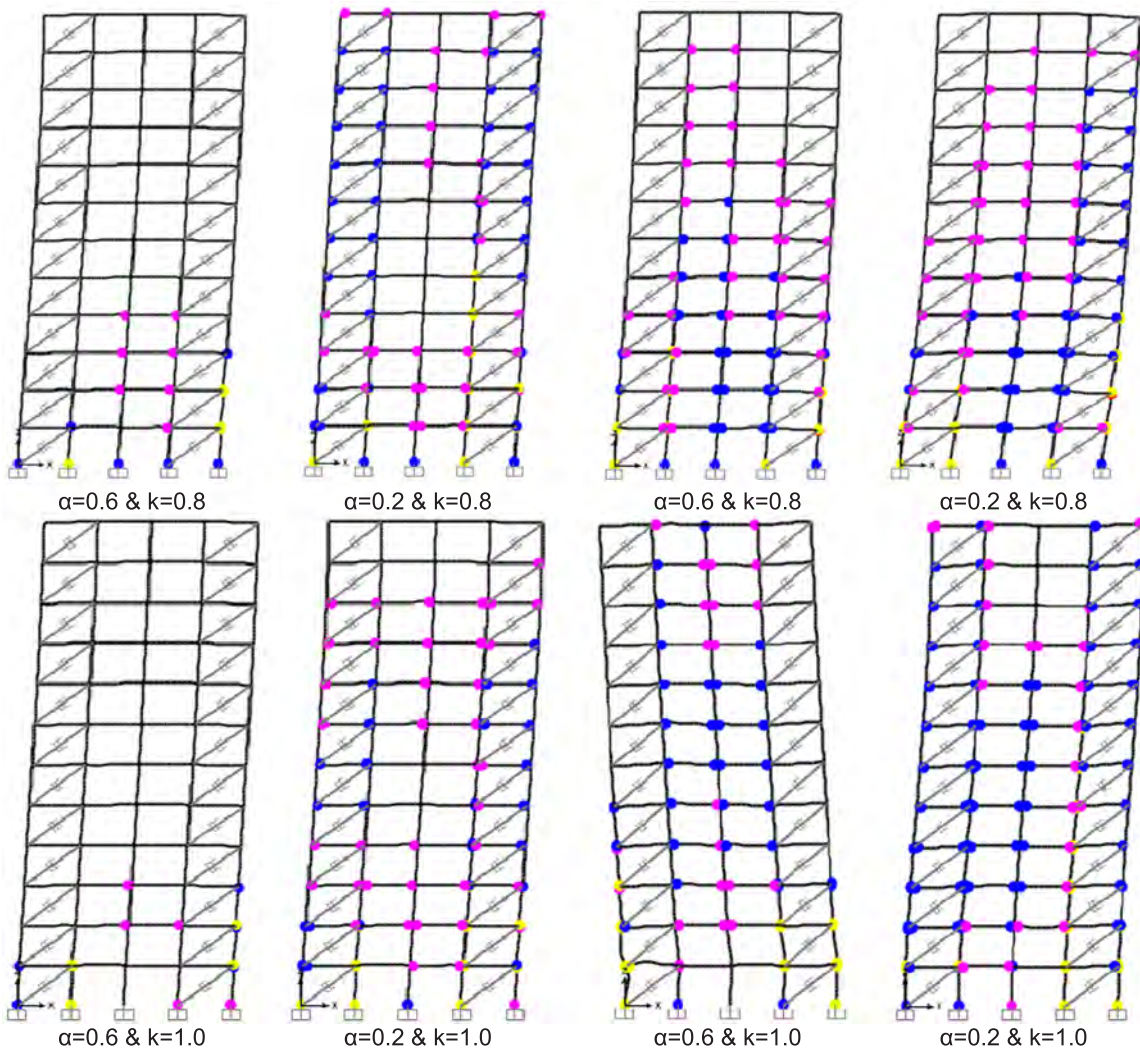


Fig. 18. Plastic hinge formations after the addition of non-linear dampers for the seismic motions No.1 (left), No.13 (upper right) and No.16 (lower right) of set II-).

storey at their bottom end; ii) the range of immediate occupancy (IO) and life safety (LS) limit states for the case of non-linear dampers with  $\alpha = 0.6$  and involve only columns of the first storey at both top and bottom ends; iii) the range of immediate occupancy (IO) and collapse (C) limit states for the case of non-linear dampers with  $\alpha = 0.2$  and

involve columns of the first two to four storeys at both top and bottom ends and many beams at several storeys.

Proceeding to set II-), Figs. 14–16, display, for  $\alpha = 1.0, 0.6$  and  $0.2$ , respectively, the height-wise variation of IDR, IV and the maximum damper forces for the two values of  $k$ . Mean values for IDR, IV and

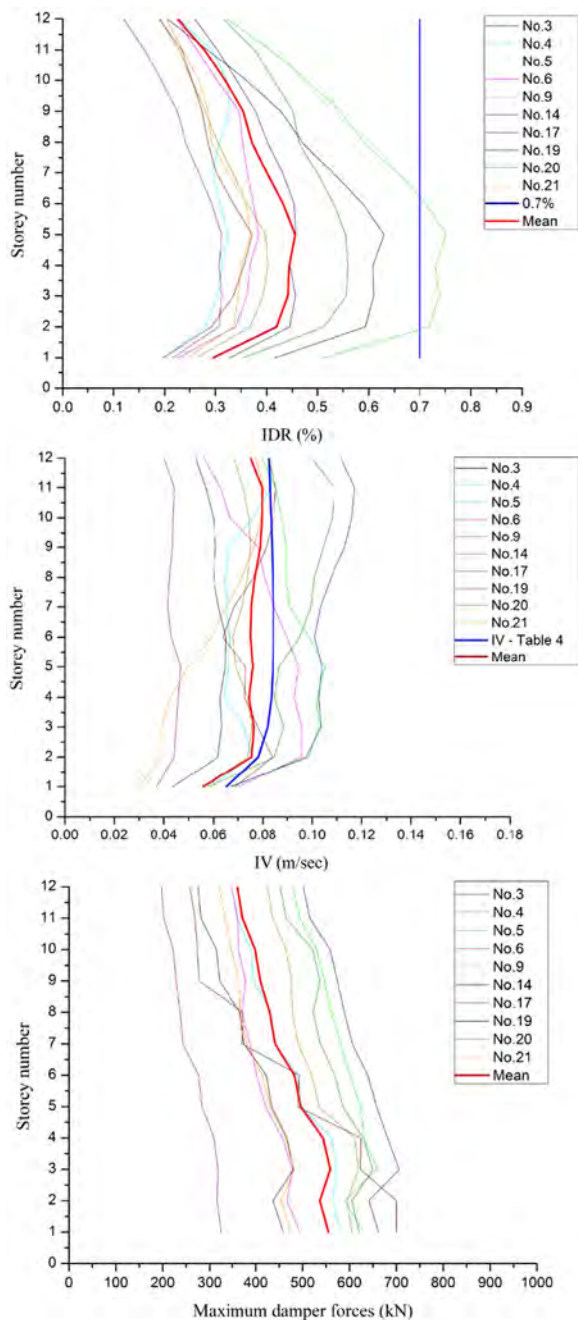


Fig. 19. IDR, IV values and maximum damper forces for  $k = 0.6$  – set I-) &  $\alpha = 0.6$ .

damper forces as well as target IDR ( $0.7\% < \text{IDR} \leq 1.5\%$ ) and IV (from Table 4) values are also shown in Figs. 14–16. Worst plastic hinges formations before and after the addition of linear and non-linear dampers, are identified for the seismic motions 1, 13, 16 and 22 of set II-) and are shown in Figs. 17–18 for the two values of  $k$ . For the case of linear dampers (Fig. 17), these worst plastic hinge formations for the seismic motions 16 and 22 are found to be the same, irrespectively of the value of  $k$ . For the seismic motion No.13 with  $k = 1.0$  and  $\alpha = 0.2$ , response cannot be computed due to excessive number of plastic hinges. From Figs. 14–18, one can conclude that: i) for the case of linear or non-linear dampers mean IDR values satisfy their target values but mean IV values do not; ii) for all damper cases, as expected, the mean maximum damper forces for  $k = 0.8$  are lower than those for  $k = 1.0$ .

For all seismic motions of set II-), the addition of dampers to the MRF is effective in reducing IDR and IV but not in reducing the number

of plastic hinges in comparison to the initial MRF without dampers. More specifically, substantial increases in axial forces of columns occurred due to the forces induced by dampers, leading to undesired plastic hinge formations at the top end of the columns of several storeys. The number of these undesired plastic hinges to columns depends on the values of  $\alpha$  and  $k$  and seems to increase as the velocity exponent decreases. End plastic rotations, according to ASCE 41–13 [14] lie within the range of immediate occupancy (IO) and collapse (C) limit states and involve columns of the first five storeys at both top and bottom ends and many beams at several storeys.

On the basis of the preceding response results for both sets and their corresponding discussion, it can be said that for set I-) the proposed IV equation, provides a good estimate towards the mean IVs of the MRF retrofitted with linear dampers or non-linear dampers with  $\alpha = 0.6$ , whereas fails to do so for the case of non-linear dampers with  $\alpha = 0.2$ . Therefore, the proposed IV equation may give a good estimate towards sizing (force capacity) of dampers with  $\alpha = 0.6$  and 1.0. Set II-) represents a higher seismic demand level than set I-), and the proposed IV equation seems to provide acceptable estimates of IVs for the cases of dampers with  $\alpha = 0.6$  and 1.0, but only for the seismic motions No.7, 10, 12 and 18.

Contrary to what is established in literature regarding limitation of maximum damper forces when non-linear dampers are used, e.g., Symans et al. [20], Martinez-Rodrigo and Romero [24], the use of IV in sizing dampers reveals that damper forces are not always reduced if non-linear dampers instead of linear ones are used. This finding may be even more pronounced in the case of stiffer MRFs that essentially respond to seismic excitation with small IDRs and IVs.

For both sets of seismic motions used herein, the addition of dampers to the MRF cause increases in axial forces of columns. If these increases are substantial, they inevitably lead to major plastic hinge formations at the top and bottom ends of the columns of several storeys. These increases have been noted in literature for steel MRFs equipped with linear and non-linear viscous dampers [23–25] and seems to be more pronounced in the case of non-linear dampers with low velocity exponent where damper forces are in phase with the structural (column) forces. Of course not only the velocity exponent but also the level of inelastic response, non-proportional damping (due to non-uniform damper placement) and bracing / connection of dampers to the structural framing can be also contributing factors towards the phase relation between structural and damping forces [20].

Thus, these increases in axial forces of columns and the subsequent plastic hinge formations should be viewed with caution in view of i) possible soft storey formation; ii) strengthening of columns and foundations; iii) collapse assessment [21,22,26] and iv) violation or modification of capacity design rules [19,26]. The proposed IV equation cannot handle these increases in axial forces of columns due to dampers and this is a matter that should be handled along the lines of the overall frame retrofit. However, it seems that these increases and the subsequent undesired plastic hinge formations to columns start to appear at an IV range of 0.065–0.085 m/sec and alter the inelastic response.

The use of a specific value for  $k$  may be important for the case of non-linear dampers where the aforementioned phase between structural and damping forces takes place. The value selected for  $k$  has direct impact on IVs and damper forces, depending on the value of  $\alpha$  and on the level of seismic demand (Figs. 9–11 and 14–16 for sets I- and II-, respectively). In fact, its impact can be even more crucial as it can be observed in Fig. 19. In this figure for set I-) and considering  $k = 0.6$  and  $\alpha = 0.6$ , the IV equation of Table 4 provides better estimate towards mean IVs and, thus, sizing (force capacity) of dampers in comparison with the cases of  $k = 0.8$  or 1.0 and  $\alpha = 0.6$  (Fig. 10). Worst plastic hinge formations for  $k = 0.6$  and  $\alpha = 0.6$  are identical with those of Fig. 13 for  $k = 0.8$  and  $\alpha = 0.6$ . On the other hand, such an improvement on IVs is obtained neither when using  $k = 0.6$  and  $\alpha = 0.6$  for set II-) nor when using  $k = 0.6$  and  $\alpha = 0.2$  for both sets. Nevertheless, it is deemed that for some cases of non-linear dampers, a lower or even

higher values of  $k$  than the 0.8 and 1.0 considered herein may lead to improved IVs, in accordance to the target IVs, but this is a matter of the steel MRF under study in conjunction with the possible significant increases in axial forces of columns due to dampers.

## 6. Synopsis and future needs

In this work expressions that provide an easy and quick estimation of IV for specific IDR levels are proposed for plane steel MRFs. The proposed expressions have a good correlation with the upper and lower limits of these limit IDR levels.

The IV expressions, corresponding to these specific IDR levels, are then employed in a seismic retrofit procedure for a plane steel MRF in which viscous dampers are inserted. The retrofit is performed for two levels of seismic demand (in terms of mean acceleration spectra) and targets for each one a specific IDR range. The damping coefficients of either the linear or the non-linear viscous dampers used for retrofit are obtained using the IV expressions given for the target IDR. The retrofitted with dampers steel MRF is subjected to non-linear time history analyses and response results in terms of IDRs, IVs and maximum damper forces are computed, involving their mean values.

From the results found, it is concluded that for one of the two levels of seismic demand, the proposed IV expression provides a good estimate of the IVs and, thereby, of the size (force capacity) of linear dampers ( $\alpha = 1.0$ ) and non-linear dampers ( $\alpha = 0.2$  and  $0.6$ ), under the consideration that these dampers are designed to resist 80–100% of the storey shear force. On the other hand, for the two levels of seismic demand and all cases of dampers, mean IDRs are within the targeted values.

The results presented herein are representative of the steel MRF studied and cannot be directly adapted to other plane or space steel MRFs. Therefore, more numerical analyses involving various combinations of plane and space steel MRFs and linear or non-linear dampers are needed for testing and calibration of the proposed IV expression. In these analyses, the placement and configuration of the dampers as well as the percentage of story shear force to be resisted by them should be investigated. Verification of the efficiency of the dampers should also include damper stroke in conjunction with IV and damper forces. Finally, further bounds on the proposed IV expression for specific IDR levels may be applied, tracing the range of IVs where damper forces provoke major plastic hinge formations to the columns of the retrofitted frame.

## References

- [1] Adachi F, Fujita K, Tsuji M, Takewaki I. Importance of interstorey velocity on optimal along-height allocation of viscous oil dampers in super high-rise buildings. *Soil Dyn Earthq Eng* 2013;56:489–500.
- [2] ASCE 7-10. Minimum design loads for buildings and other structures. Virginia, USA: American Society of Civil Engineers; 2010.
- [3] Palermo M, Silvestri S, Landi L, Gasparini G, Trombetti T. Peak velocities estimation for a direct five-step design procedure of inter-storey viscous dampers. *Bull Earthq Eng* 2016;14:599–619.

- [4] Palermo M, Silvestri S, Trombetti T. On the peak inter-storey drift and peak inter-storey velocity profiles for frame structures. *Soil Dyn Earthq Eng* 2017;94:18–34.
- [5] Hatzigeorgiou GD, Papagiannopoulos GA. Inelastic velocity ratio. *Earthq Eng Struct Dyn* 2012;41:2025–41.
- [6] Hatzigeorgiou GD, Pnevmatikos NG. Maximum damping forces for structures with viscous dampers under near-source earthquakes. *Eng Struct* 2014;68:1–13.
- [7] Pekcan G, Mander JB, Chen SS. Fundamental considerations for the design of non-linear viscous dampers. *Earthq Eng Struct Dyn* 1999;28:1405–25.
- [8] Favvata MJ. Minimum required separation gap for adjacent RC frames with potential inter-storey seismic pounding. *Eng Struct* 2017;152:643–59.
- [9] Karavasilis TL, Bazeos N, Beskos DE. Drift and ductility estimates in regular steel MRF subjected to ordinary ground motions: a design-oriented approach. *Earthq Spectra* 2008;24:431–51.
- [10] Papagiannopoulos GA, Beskos DE. Towards a seismic design method for plane steel frames using equivalent modal damping ratios. *Soil Dyn Earthq Eng* 2010;30:1106–18.
- [11] Logotheti VE. Seismic retrofit of steel frames with non-linear viscous dampers using interstorey velocity [M.Sc. Thesis]. Greece: Department of Civil Engineering, University of Patras; 2018.
- [12] Eurocode 3. Design of steel structures – Part 1-1: General rules and rules for buildings. Brussels: CEN; 2009.
- [13] Eurocode 8. Design of structures for earthquake resistance – Part 1: General rules, seismic actions and rules for buildings. Brussels: CEN; 2009.
- [14] ASCE 41-13. Seismic evaluation and retrofit of existing buildings. Virginia, USA: American Society of Civil Engineers; 2014.
- [15] SAP2000. Static and dynamic finite element analysis of structures, Version 19.2.1, Computers and Structures. Berkeley, California, USA; 2017.
- [16] Loulelis DG, Papagiannopoulos GA, Beskos DE. Modal strength reduction factors for seismic design of steel moment resisting frames. *Eng Struct* 2018;154:23–37.
- [17] Taylor Devices. 2016. <<http://taylordesdevices.com/pdf/2016/01Jan/DamperLUDsizesPDF2.pdf>>.
- [18] Wang S, Mahin SA. Seismic retrofit of a high-rise steel moment-resisting frames using fluid viscous dampers. *Struct Des Tall Spec Build* 2017;26:e1367.
- [19] Kariniotakis KK, Karavasilis TL. Modified capacity design rule for columns in tall steel MRFs with linear viscous dampers within the framework of Eurocode 8. *Bull Earthq Eng* 2018;16:917–32.
- [20] Symans MD, Charney FA, Whittaker AS, Constantinou MC, Kircher CA, Johnson MW, McNamara RJ. Energy dissipation systems for seismic applications: current practice and recent developments. *J Struct Eng* 2008;134:3–21.
- [21] Miyamoto HK, Gilani ASJ, Wada A, Ariyaratana. Limit states and failure mechanisms of viscous dampers and the implications for large earthquakes. *Earthq Eng Struct Dyn* 2010;39:1279–97.
- [22] Miyamoto HK, Gilani ASJ, Wada A, Ariyaratana. Identifying the collapse hazard of steel special moment-frame buildings with viscous dampers using FEMA P695 methodology. *Earthq Spectra* 2010;27:1147–67.
- [23] Uriz P, Whittaker AS. Retrofit of pre-Northridge steel moment-resisting frames using fluid viscous dampers. *Struct Des Tall Spec Build* 2001;10:371–90.
- [24] Martinez-Rodrigo M, Romero ML. An optimum retrofit strategy for moment resisting frames with nonlinear viscous dampers for seismic applications. *Eng Struct* 2003;25:913–25.
- [25] Seo CY, Karavasilis TL, Ricles JM, Sause R. Seismic performance and probabilistic collapse resistance of steel moment resisting frames with fluid viscous dampers. *Earthq Eng Struct Dyn* 2014;43:2135–54.
- [26] Labise CC, Rodgers GW, MacRae GA, Chase JG. Viscous and hysteretic damping – impact of capacity design violation in augmented structural systems. *Bull NZ Soc Earthq Eng* 2012;45:23–30.

## Further reading

- [1] Kitayama S, Constantinou MC. Seismic performance of buildings with viscous damping systems designed by the procedures of ASCE/SEI 7-16. *J Struct Eng* 2018;144. [04018050-1–04018050-14].